

Hover kinematics and distributed pressure sensing for force control of biorobotic fins*

Jeff C. Kahn, Jr., Brooke E. Flammang, James L. Tangorra, *Member, IEEE*

Abstract— A comprehensive understanding of the ways in which fish create and control forces is fundamental to engineering underwater vehicles that maneuver with the agility of fish. In this study the sunfish was selected as a biological model from which to understand pectoral fin motions and forces during hover. The kinematic patterns of the biological fin were identified and implemented on a biorobotic model of the fin. The effects of fin patterns and mechanical properties on force were evaluated. Pressure was measured at multiple points on the fin's surface and assessed for use in the closed loop control of fin force. The study revealed that a wide range of motions are used during hover, and that forces are significantly different from those found previously for steady swimming. However as fin speeds increase, the fin's dynamic motions, and the magnitude and direction of the forces become more similar to those of steady swimming. Collective measures of pressure over the fin's surface exhibited trends that correlated well with fin forces in relative magnitudes and directions. Results strongly suggest that distributed measures of pressure are useful for force prediction and control.

I. INTRODUCTION

Bony fish are extraordinary agile swimmers and can serve as biological models from which to understand how hydrodynamic forces are created and controlled with fins. Their agility comes from their ability to control their movements with multiple fins, and this agility often far exceeds that of engineered underwater vehicles [1]. These fins create forces on the body through repeated kinematic patterns, or gaits. These gaits are used to produce characteristic forces that drive the locomotive behavior of fish (e.g. a steady swimming gait is primarily thrust producing for swimming forward in flow). The bluegill sunfish (*Lepomis macrochirus*), uses its pectoral fins to produce a variety of gaits, such as steady forward swimming, yaw turn maneuvers, and hovering in place. Hover is an interesting gait from a force production standpoint because the sunfish is dynamically unstable; constant force production is necessary to keep the fish center of mass balanced atop the center of buoyancy. Whereas motions such as steady swimming and turning maneuvers rely on a dominant pattern to produce characteristic forces, hover has a

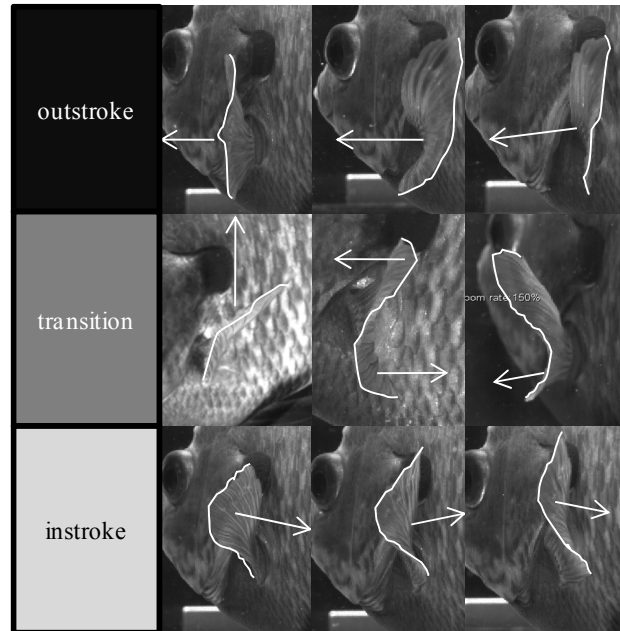


Figure 2. Sunfish (TOP) and biorobotic fin (BOTTOM) executing the dominant hover motion of “Ventral led cupping” outstroke to “Flat Plate Lift and Drop” instroke. Robotic fin trajectories were derived by point and velocity tracking of the fin segments through 3D high speed video and mapping of trajectories to the degrees of freedom on the robot. Robotic trajectories were consistent with sunfish fins through time varying curvature and velocities of fin regions.

wide repertoire of fin motions used to maintain posture that vary significantly in trajectory, velocity, and direction.

Finer levels of fish agility emerge through the control of properties within a particular gait. Within a particular gait, the fish also can modulate forces by actively changing the kinematics and mechanical properties of its fins. By varying mechanical stiffness through co-contraction of muscles, the fin can change the magnitude of the time varying forces, and by increasing its flapping frequency both the magnitude and direction of the forces are affected. Slight changes in trajectory are also observed and likely allow the fish to “fine-tune” the forces produced through a particular cycle. These beat-to-beat differences in fin motions suggest that sensory feedback is used in controlling forces [2]. The wide repertoire of hover motions observed further supports this tuning hypothesis (Fig. 1). Neurobiological studies are just beginning to address how this sensory feedback works in aquatic vertebrates. Sensory nerve fibers densely innervate the pectoral fins in regions of crucial to the development of forces [3], though the nature of the feedback (i.e. cell body types, physical phenomena measurable) is largely unknown.

To the authors' knowledge, there have been no biological studies that address the kinematics or forces of hovering fish.

* Research supported in part by ONR N00014-09-1-0352, NSF EFRI 0938043, and DOE GAANN P200A100145.

J.C. Kahn, Jr. is with the Laboratory for Biological Systems Analysis, Drexel University, Philadelphia, PA 19104 USA. (ph 215-895-2993, fax 215-895-1468, e-mail: kahn@drexel.edu).

B.E. Flammang is with the Department of Organismic and Evolutionary Biology, Harvard University, Cambridge, Massachusetts USA. (e-mail: bflammang@post.harvard.edu).

J.L. Tangorra, is with the Laboratory for Biological Systems Analysis, Drexel University, Philadelphia, PA 19104 USA. (e-mail: tangorra@coe.drexel.edu).

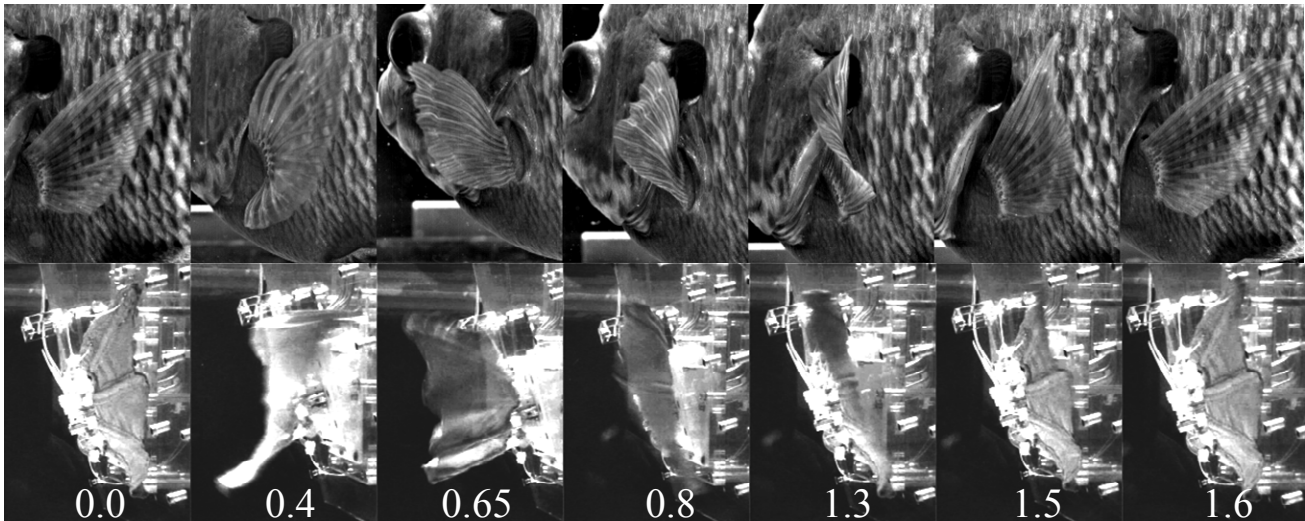


Figure 2. Sunfish (TOP) and biorobotic fin (BOTTOM) executing the dominant hover motion of “Ventral led cupping” outstroke to “Flat Plate Lift and Drop” instroke. Robotic fin trajectories were derived by point and velocity tracking of the fin segments through 3D high speed video and mapping of trajectories to the degrees of freedom on the robot. Robotic trajectories were consistent with sunfish fins through time varying curvature and velocities of fin regions.

Pectoral fin use in steady forward swimming [4], varied fin maneuver motions, and escape reflexes [5] have all received kinematic and force analysis through modeling and physical testing. Behavioral biology work has long documented the value of hovering as a means for foraging, hunting, socialization, and nest guarding behaviors [6] but the role of specific pectoral fin motions to produce biologically derived hover forces is a novel consideration. This study implements observed sunfish kinematics during hover to provide the first analysis of forces during hovering.

Robotics studies have developed hovering vehicles, and have significantly analyzed forces on engineered hover motions [7],[8], but have never before implemented a biologically-derived hover motion on a robotic platform with flexible fins. And further, despite neurobiological evidence in aquatic and terrestrial vertebrates, few robotics studies have considered distributed measurements along the limbs and surfaces responsible for propulsion. Biologically derived distributed sensory systems have been considered, including notably an artificial lateral line for measurements of local flow [9] and electroreceptive sensors to model a ghost knifefish [10], but few studies have examined fin-intrinsic sensation on robotic fin models [11].

Previous experiments with a flexible biorobotic model of the bluegill sunfish fin have evaluated a steady swimming gait [11] and a yaw turn maneuver [12] and how kinematic and mechanical properties affect force production through these modes [13]. Studies using computational fluid dynamics have also verified the fin mechanisms of force production [4]. Prior work with the biorobotic model has addressed fin bending as a sensory measure for estimation of forces, but found that bending alone could not be used to estimate the magnitude of force produced [11].

In this study, sunfish pectoral fin hover kinematics are analyzed in groups of outstroke/instroke features, and then in kinematic patterns. Secondly, the kinematics are applied to a biorobotic pectoral fin to evaluate the forces produced during hover. Third, the effects of changing fin kinematics and

mechanical properties on these forces is determined. Lastly, distributed measures of pressure over the robotic fin’s surface are assessed as a means to predict the time-varying propulsive force for control of the fish body.

II. METHODS

A. Biological hover motions

Studies of bluegill sunfish hovering were conducted in a 600 L flow tank with a 26cm by 26cm by 80cm working volume as in previous research [14], [15]. Three synchronized high-speed video cameras (Photron USA, San Diego, CA, USA) were positioned to record simultaneously the fish swimming in the lateral (XY plane), posterior (YZ plane) and ventral (XZ plane) views. Videos of the fish hovering were filmed at 250 frames s⁻¹ with 1024 by 1024 pixel resolution. Hovering video was taken in static water.

Ethogram techniques developed from [16] were employed to classify the fin patterns observed through hover videos. Following the identification of a probabilistically important cycle of hover, the video views of this fin beat were calibrated in three dimensions using direct linear transformation of a custom 20-point calibration frame and digitized using a program written for MATLAB 7 (MathWorks, Natick, MA, USA) by Ty Hedrick [17]. Points along the biological fin were fit to the robotic fin base using a least squares regression to fit the three base points of each digitized fin ray to a line segment that extended through a center of rotation on the robot. Angles of rotation were calculated for the available robot degrees of freedom and these angles through time formed the trajectories of the programmed hover motion. Individual fin-ray trajectories were fit to eighth-order sinusoidal basis functions that were tuned to capture relevant visual features of the hover motion as determined by ethogram.

B. Biorobotic hover and fin pressure studies

The biorobotic pectoral fin was supported by an air bearing carriage (New Way S301301, New Way Air

Bearings, Aston, PA) and fixed against two s-beam load cells (LSB200, FUTEK, Irvine, CA) to measure force in thrust and lateral directions. A 10 point linear calibration was applied before experiments. More details of the setup are described in [18], [11]. The pectoral fin membrane (80% polyester, 20% elastane) was sewn from a 4x scaled pattern of a sunfish pectoral fin. Previous work used this material untreated but we reasoned that this porous material would confound pressure measurements between outer and inner fin faces [19]; therefore the fin was coated with two thin coats of latex paint (Liquid Latex Body Cosmetic, Maximum Impact, Langhorne, PA) and cured for waterproofing.

To execute the kinematic patterns on the robot, the fitted functions were sent as commands through servomotors to each of the seven segments of the fin, called fin rays. Each fin ray executed a sweep trajectory from a hinge joint at its base, and 3 of 5 of the fin rays executed lateral movement by rotation about an aluminum pin. The rays were actuated with low stretch tendons routed to digital servomotors (HSR-5990TGs, Hitec RCD USA, Poway, CA) above the water line as in [4].

High precision catheter-style pressure sensors (SPR-524, Millar Instruments, Houston, TX) were placed on the fin at areas with high sensory innervation in the sunfish (as in [3]). These sensors are manually calibrated in a signal conditioning unit (PCU-2000, Millar Instruments, Houston, TX) before each test and provide accuracy within 1% and a frequency response up to 1kHz. These sensors were used to measure pressure on the inner and outer faces of the fin along the dorsal and ventral leading edges. The sensors were oriented orthogonally to the fin face, and affixed to the webbing using the aforementioned latex paint. Since the sensors measured total pressure, including hydrostatic pressure change due to depth, testing protocol was setup to allow for long pauses between outstroke and instroke to obtain the DC offset in the pressure due to depth change. This hydrostatic value was subtracted from measures of pressure to obtain an estimate of the dynamic pressure changes on the fin surface.

To evaluate the force production of hover and to determine if on-fin pressure measurements are predictive of the magnitude of forces through varied swimming conditions, the pectoral fin was programmed to execute steady swimming with full factorial experiments varying fin ray stiffness (200,400,600,800,1000x) and fin beat period ($T = 4.00, 2.00, 1.54, 0.77, 0.62$ s) as on-fin pressure data were taken with 8 pressure sensors at the dorsal and ventral leading edges of the fin's outer and inner surfaces at locations distal and proximal to the fin base. Data were taken at 100Hz using real-time data acquisition software programmed in LabVIEW and compiled on a dedicated hardware controller (LabVIEW 2010 and PXI-8106, National Instruments, Austin, TX).

III. RESULTS

A. Biological hover motions

The analysis of fin motions revealed that sunfish use a range of kinematic patterns during hover. Certain motion patterns occur much more frequently than others, but unlike the repeated gait used during steady swimming [20], the hover gait cannot be characterized as a single motion

program. Instead, the ethogram analysis characterized pectoral fin motions during hover into twelve motion patterns; six for the fin's outstroke from the body, two for the fin's instroke to the body, and four for the transition from outstroke to instroke (Fig. 1).

Six characteristic motion patterns were identified for the outstroke of the fin from the body, three of which accounted for 71% of the outstroke motions analyzed. The most common motion pattern ($P = 25\%$) was an asymmetric cupping of the fin about its centerline (from root to distal end) with the cupping led by the fin's ventral edge (ventral led cupping, Fig. 2). The second characteristic pattern ($P = 23\%$) was a symmetric cupping motion (cupping), which was led approximately equally by the dorsal-and ventral-most fin rays. In both the "cupping" and the "ventral led cupping" patterns, the cupped shape of the fin extended from the fin's root to the fin's distal edge. These two cupping patterns are similar to the cupping and sweep motion that dominates the pectoral fin's motion during steady swimming [20]. The third most common outstroke pattern ($P = 21\%$, cupping with flat plate) was defined by a more moderate cupping of the fin at its base with a flattening of the fin towards its distal edge. There was almost no phase difference between the fin rays at their distal ends and this resulted in the fin appearing flat as it moved through the water. Three additional motion patterns were observed less frequently. These were descriptively named "dorsal lead" ($P = 10\%$), "flat plate" ($P = 10\%$), and "half stroke" ($P = 9\%$).

Instroke motions were characterized by two patterns. The most frequent ($P = 83\%$) was a motion where the fin moved as a flat plate, but did not follow a straight trajectory back to the body. The fin moved toward the body and dorsally during the first half of the instroke, and toward the body and ventrally during the second half of the instroke (flat plate lift and drop, Fig. 2). Much less frequent ($P = 17\%$) was an instroke pattern that was led by the dorsal-most fin ray and that had linearly increasing phase lag between subsequent fin rays.

Transition motions were short duration movements that allowed the fin to transition from the outstroke to the instroke pattern. These motions usually included either a sudden deceleration or change in direction of groups of fin ray. Most common ($P = 55\%$) was an "s-undulation" (Fig. 1) of the rays where the ventral half of the fin changed direction rapidly and the dorsal segment moved toward the midline and before changing direction, inward, producing an "S" shape. Three more observed transition patterns occurred much less frequently than the "s-undulation". These were descriptively named "inversion" ($P = 15\%$), "spread" ($P = 15\%$), and "upward flap" ($P = 15\%$, Fig. 1).

B. Biorobotic hover

1) Fin motions

The biorobotic fin was programmed to execute the "ventral led cupping" pattern for its outstroke, the "flat plate lift and drop" for its instroke, and no transition between the outstroke and instroke. This motion program represented the most frequent pattern exhibited by the sunfish during hover. The robotic pectoral fin captures major components of the biological fin's motion when the robot's fin rays were scaled between 200 and 1000 times the flexural rigidity of the

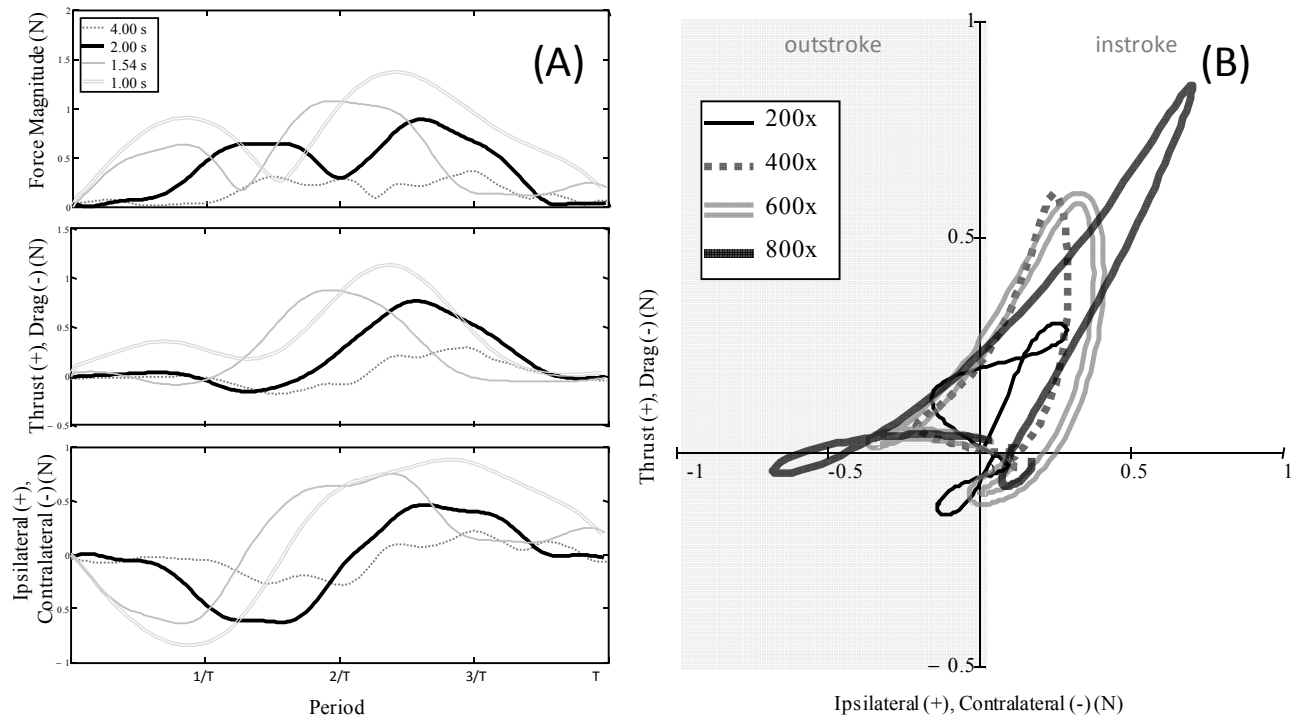


Figure 3. Characteristic forces of hover in the thrust-lateral directions. 2D magnitude of force (A.TOP), thrust force (A.MIDDLE), and lateral force (A.BOTTOM) are graphed as flapping frequency is varied from 0.25 to 1.00Hz. Forces representative of hover in the biology would typically be executed at 0.50Hz (highlighted) and slower. Forces shown in the thrust-lateral plane (B) through varied stiffnesses show the characteristic representative forces through one fin beat (outstroke to instroke) and allow envisioning of body movement in the thrust-lateral plane. Through the outstroke a strong force is mostly directed laterally, whereas the instroke motion creates strong forces in the thrust and lateral directions. Data are representative of a six-cycle average of the forces were low-pass filtered at 5Hz for clarity.

biological fin rays. In general, as the fin moved away from the body in the outstroke (Fig. 2; $t=0.0,0.4$ s), the ventral region of the fin remained stiff as it led the motion, followed by the dorsal leading edge. The robotic fin motion experienced significant bending at the distal tips of the dorsal leading edge and the overall curvatures were consistent with the sunfish's fin curvatures. As the "ventral led cupping" pattern continued, the ventral edge lifted up toward the dorsal leading edge to bring the distal fin tips closer together. Through this time period, the robotic fin did not have as much dorsal movement as the biological fin in the medial rays. This was due to having only a single degree of freedom in medial fin rays as compared to two degrees of freedom in ventral and dorsal rays.

Beginning the outstroke "flat plate lift and drop motion", the ventral edge started to drop downward (Fig. 2; $t=0.65, 0.8$ s), leading the motion and creating a flattened appearance along the edge of the fin with some bending at dorsal and medial fin tips. At low flexural rigidities (200x, 400x, 600x), the curvature of the robot visually matched the fish fin curvature but at higher rigidities (800x, 1000x), pockets tended to form in the fin webbing that caused the fin edge to appear wavy rather than flat. As the instroke completed, the ventral edge met the body (Fig. 2; $t=1.3$ s) before the dorsal edge (Fig. 2; $t=1.5$ s) in both robot and fish. The motion completed with a very slight rotation of both the dorsal and ventral segments downward. This last part of the motion was more irregular in the robot than the fish, as medial fin rays could not rotate about the appropriate axis to move downward. The final "drop" of the motion was approximated

by the downward rotation of the dorsal and ventral fin rays in the robot.

Though some limitations were encountered with the robot's degrees of freedom in the medial fin rays, the motions matched biological motions consistently through biologically relevant rigidities and fin beat periods and thus the programmed hover motion was validated visually as a model of sunfish hovering.

2) Hover forces

Over the conditions tested, a dominant hover force profile was identified. During the "cupping with ventral lead" outstroke, the fin produced drag and a strong contra-lateral force (Fig. 3A). As the fin transitioned from outstroke to instroke, the magnitude of the force decreased. Through the "flat plate lift and drop" instroke, the fin produced strong thrust and ipsi-lateral force. The average lateral forces were typically balanced through the fin beat such that the mean lateral force was close to zero. Mean thrust forces through the beat were typically close to zero or slightly positive depending on test conditions. The magnitude, direction, and time varying courses of the force varied as fin beat frequency and mechanical stiffness were modulated. Application of characteristic forces to the fish body would result in a backward and contra-lateral movement through the outstroke, forward and ipsi-lateral movement through the instroke, and a slight net forward movement of the body from the starting position (Fig. 3B). When coupled with the wide repertoire of other motions associated with sunfish hovering, this net result of slight forward movement and balanced lateral movement is relevant to hover behaviorally. Further, since hover

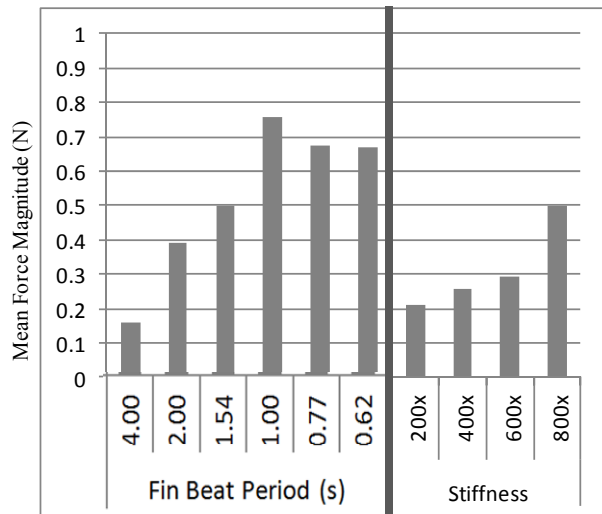


Figure 4. Force production of hover through varied stiffnesses and fin beat periods (B). For varied frequencies, data are shown from an 800x fin; for varied stiffnesses, 0.65Hz flapping frequency data were used. Each are representative of general trends through varied frequencies and stiffnesses.

motions are executed on two pectoral fins and multiple body fins, it's reasonable to assume that the contra-lateral pectoral fin and could employ a fin beat to correct for the thrust force generated.

When fin stiffness was held constant, varying the fin beat period affected the magnitude, direction, and time course of fin forces. For slow and moderate fin speeds ($T=4, 2, 1.54$, and 1 s), the mean magnitude of the 2d forces increased as the duration of the fin beat was reduced and the fin's velocity increased (Fig. 4). Effects on forces were also largely dependent on whether the fin was in the outstroke or instroke of the fin beat. At the fastest fin speeds ($T=1.54, 1.00$ s) thrust, not drag, was produced during the outstroke (Fig. 3A). The shift from drag to thrust is not, however, surprising. At faster fin speeds, the fin bends back and directs flow backwards. This behavior is consistent with steady swimming fin beat patterns, which take advantage of fin bending to produce thrust during the outstroke. During the instroke, decreasing the period increased the average lateral forces significantly, leading to larger and longer duration ipsi-lateral forces (Fig. 3A). Thrust means in the instroke also increased with decreasing beat period. The increase of thrust and contra-lateral components drove up the magnitude forces during the instroke. Changes in the fin beat period also change fish body movements. Increasing the fin beat period leads to more balanced thrust-drag components of the force and would lead to a motion in which the fish starts and ends the beat in the same global position. At shorter beat durations, the motion would tend to move the fish forward and ipsi-laterally as a net result.

When fin beat period was held constant, increasing the stiffness tended to increase mean 2d forces, change the direction of thrust forces in the outstroke, and increase mean lateral force magnitudes. As stiffness increased, the strong drag and contra-lateral forces of the outstroke transitioned to slight thrust and contra-lateral forces (Fig. 3B). Through the instroke, increasing stiffness tended to increase the mean thrust and contra-lateral forces, without impacting direction.

At very high stiffness (Fig. 3B; 800x trace) the outstroke contra-lateral and thrust forces were significantly greater than other stiffnesses. Increasing stiffness tended to cause instroke thrust and magnitudes to develop earlier in the period (Fig. 3A), but did not affect the rate of development of lateral forces. Applying forces to the fish body as fin stiffness increased would tend to move the fish more laterally during the instroke and outstroke and more forward during the instroke due to increased thrust. Biological sunfish hover forces are not currently known, but the fish body motions are consistent with the forces produced by the biorobotic fin.

C. Distributed fin pressure sensing

The fin propulsive force and the fin-intrinsic pressure measures exhibited many overlapping features in the data. Pressure and force magnitudes were highly correlated as fin conditions were altered, which suggested that pressure measures could be used to estimate the propulsive force. Pressures taken from regions of the fin trended with particular components of the propulsive force. Differences in pressure between the dorsal and ventral regions of the fin were clarified from the experiments, as well as differences between the outer and inner faces of the fin. Temporal differences in pressure and force were promising for the estimation of propulsive forces using distributed pressure measures.

Magnitude of pressure tracked with force magnitude across fin conditions. When forces were increased through modulations in stiffness and flapping frequency, the pressure magnitudes increased proportionally. This result held through all previously tested force profiles in steady swimming [11]. Most significantly, this suggests that pressure magnitudes could be used to estimate force magnitudes with a slight time lag (see below).

Dorsal and ventral leading edge pressure measures correlated with different components of the time-varying force. Pressure measures along the dorsal leading edge closely matched thrust components of force during steady swimming (Fig. 5). In steady swimming with a pause (outstroke, pause, instroke) thrust forces (Fig. 5B) followed a consistent pattern that was matched by the dorsal leading edge pressure sensors (Fig. 5D). During the outstroke, small thrust forces developed with positive increases in dorsal pressures. As the outstroke completed, a large peak of drag force developed as a large negative pressure peak developed. Through the instroke, as the fin was flapped back to the body, only thrust was created, just as only positive pressures were seen on the dorsal leading edge. Ventral edge pressure measures captured features from both the thrust and lateral components of force. A comparison of the signals in lateral force (Fig. 5C) and ventral pressure (Fig. 5F) showed that oscillations in the lateral forces (due to wave reflections in a small tank) were measured in the ventral edge sensors. Additionally, these sensors did exhibit a small negative peak during the instroke that is only seen on the lateral force trace (Fig. 5D,F).

The dorsal leading edge did not generally support a pressure difference across the outer and inner faces (Fig. 5D,E), but the ventral leading edge did (Fig. 5F). Across all experiments, pressure measures on paired dorsal leading edge sensors (same location, inner and outer faces) were nearly

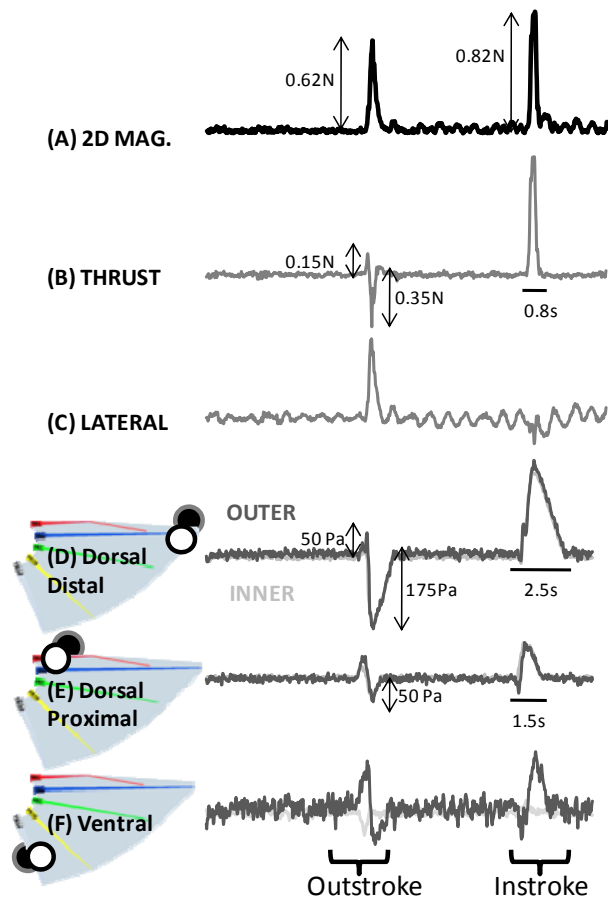


Figure 5. Distributed pressure measurements on the biorobotic fin during steady swimming measure varied aspects of the force. Dorsal distal sensors (D) trend closely with the magnitude and direction of thrust forces (B). Dorsal proximal sensors (E) also trend with thrust forces (B), but are lesser in average magnitude than their distal counterparts, suggesting development of higher pressures along the length of the fin. Ventral sensors (F) tend to exhibit similar oscillatory noise to the lateral forces (C). Dorsal sensors (D,E) do not tend to support a pressure difference across the fin whereas ventral sensors (F) frequently do. These representative data are from a steady swimming fin at 1.00Hz flapping frequency with 800x fin stiffness. Large oscillations in the lateral forces (C) were a result of reflected waves in the static testing tank.

identical in magnitude and direction. It is likely that the stiffness of the ventral edge coupled with more limited movement (dictated by length and kinematics) allowed for a pressure difference to be supported across the webbing. Pressure measures along the length of the ventral leading edge were not significantly different across testing conditions. Since the flexural rigidity is held constant across this very short segment of the fin, it is unlikely that the bending or forces felt here could differ along the length. This result suggests that one pressure sensor pair (inner and outer faces) could serve as a "representative" measurement for a larger region of the fin.

Along a single fin ray, pressure magnitudes increased as the distance from the fin base increased. Additionally, these more distant pressure events had a longer signal duration (Fig. 5D,E; 1.5s, 2.5s). Along the dorsal leading edge the proximal pressure signals were significantly lower in magnitude than the distal pressure signals (Fig. 5D,E). Visual

study of the vortex development showed that the vortex size increased along the length of the leading edge, which supports the hypothesis of stronger fluidic events near the fin tips.

The timing of pressure and force signals was useful for understanding the physical relationships between pressure and force on the fins. Pressure signal events occurred prior to force signal events. Gross changes in pressure (e.g. a large positive peak) typically developed 5-10 ms before similar changes in force. This result suggests that fin pressures could be used to predict propulsive force, but further testing is required. There was a smaller difference (~1ms) in pressure development from proximal to distal segments along the length of a single fin ray. The duration of pressure events was significantly longer than the duration of force events. Pressure signals typically had longer duration than force signals by a factor of 1.5 or greater, measured by the change of the signal from the constant DC value (Fig. 5B,D,E; time markers). This likely had to do with the added mass to the fin during swimming; forces did not develop fully until stored energy was released into the flow. However, pressure developed long past entire duration of the stroke (1.5T vs 1.0T; with T as the fin beat period), thus resulting in longer pressure events than force events.

IV. CONCLUSION

A frequently occurring pattern of sunfish hovering was evaluated on a biorobotic pectoral fin platform for the first time and dominant patterns of forces were identified in the thrust-lateral planes. The developed gait produced consistent forces that can be varied with kinematic and mechanical properties to produce patterns of force consistent with the biological behavior of hovering. This result opens pathways for further research in gait-based closed loop force control of fins and expands the testable repertoire of motions and resulting forces for the pectoral fin robot. Future studies will utilize the hover motion with a multiple fin fish robot and with paired robotic pectoral fins to consider interactions between fins during the complex gait.

Sunfish pectoral fin hovering was analyzed and a repertoire of hover motions were extracted using ethogram techniques. A significant result was the evidence that hover is executed with much more stroke-to-stroke variation than other gaits, and this has significant bearing for engineers of finned robotic systems and aquatic bio-inspired designs that have often relied on consistent, dominant motions to produce forces. With this growing repertoire of fin gaits, small kinematic pattern variation can be used to generate desired forces through a fin beat. For instance, to generate drag and balanced lateral forces, the fin could execute the "ventral led cupping" at a slow speed and a "flat plate lift and drop" at a higher speed. Even though the forces of "hover" were considered through varying kinematic and mechanical properties and clear trends were identified, hovering is a much more complex behavior with multiple patterns of outstroke, transition, and instroke that serve to maintain fish body balance and position. These beat-to-beat variations are also highly indicative of a sensory based control that regulates motion patterns within hover. Future work will address the specific roles of these patterns and how they

contribute to the fine tuning of forces and closed-loop control of the fish body. Further, with a library of known force profiles, force-control algorithms can be learned using machine learning classification techniques.

Lastly, a distributed fin-intrinsic pressure system was instrumented on a biorobotic pectoral fin and tested through varied fin kinematics and mechanical properties, showing direct relationships to the fin's propulsive forces. Expanding on experiments with single pressure measures [19], this study showed how individual sensors could be used to estimate instantaneous forces on the body and that multiple sensors could be used to estimate mean force magnitudes through an entire cycle. Trends observed showed promising results for the closed-loop control of fins as gaits, mechanical properties, and kinematics vary during swimming. Measuring distributed pressures on force producing surfaces is likely to be a valuable for force estimation in many other types of robotic systems and could be a possible link to understanding fish strategies of sensory input. Sensory based control algorithms will likely require distributed multi-modal sensing that includes measures of fin pressure and ray curvature.

Control of flexible robotic fins will be highly dependent on successful estimation of the propulsive forces. Distributed pressure sensing could be used in conjunction with distributed bending sense to produce estimates of propulsive force. With distributed bending data, the curvature of the fin can be estimated, and with this knowledge it becomes possible to estimate many features of the fin (outstroke/instroke, velocity, local curvatures, stiffness). Given this information, local pressure measures can be weighted to estimate total propulsive force. Since early studies show that local pressures trend with aspects of the propulsive force in magnitude and direction, a weighting of these signals will likely produce accurate estimates of force in real time.

ACKNOWLEDGMENT

The authors thank George Lauder and the many members of the Lauder and Tangorra laboratories.

REFERENCES

- [1] P. R. Bandyopadhyay, "Maneuvering Hydrodynamics of Fish and Small Underwater Vehicles," *Integrative and Comparative Biology*, vol. 42, pp. 102-117, 2002.
- [2] D. H. Thorsen, et al., "Swimming of larval zebrafish: fin-axis coordination and implications for function and neural control," *Journal of Experimental Biology*, vol. 207, pp. 4175-4183, November 15, 2004.
- [3] D. H. Thorsen and M. E. Hale, "Neural development of the zebrafish (*Danio rerio*) pectoral fin," *The Journal of Comparative Neurology*, vol. 504, pp. 168-184, 2007.
- [4] G. V. Lauder, et al., "Locomotion with flexible propulsors: I. Experimental analysis of pectoral fin swimming in sunfish," *Bioinspiration & Biomimetics*, vol. 1, p. S25, 2006.
- [5] P. Domenici and R. Blake, "The kinematics and performance of fish fast-start swimming," *Journal of Experimental Biology*, vol. 200, pp. 1165-78, April 1, 1997.
- [6] R. W. Blake, "The Energetics of Hovering in the Mandarin Fish (*Synchropus Picturatus*)," *The Journal of Experimental Biology*, vol. 82, pp. 25-33, October 1, 1979.
- [7] N. Kato and M. Furushima, "Pectoral fin model for maneuver of underwater vehicles," in *Autonomous Underwater Vehicle*

- Technology, 1996. AUV '96., Proceedings of the 1996 Symposium on, 1996, pp. 49-56.
- [8] P. E. Sitorus, et al., "Design and Implementation of Paired Pectoral Fins Locomotion of Labriform Fish Applied to a Fish Robot," *Journal of Bionic Engineering*, vol. 6, pp. 37-45, 2009.
- [9] Y. Yang, et al., "Artificial lateral line with biomimetic neuromasts to emulate fish sensing," *Bioinspiration & Biomimetics*, vol. 5, p. 016001, 2010.
- [10] M. A. MacIver, et al., "Designing future underwater vehicles: principles and mechanisms of the weakly electric fish," *Oceanic Engineering, IEEE Journal of*, vol. 29, pp. 651-659, 2004.
- [11] C. Phelan, et al., "A biorobotic model of the sunfish pectoral fin for investigations of fin sensorimotor control," *Bioinspiration & Biomimetics*, vol. 5, p. 035003, 2010.
- [12] J. R. Gottlieb, et al., "A biologically derived pectoral fin for yaw turn manoeuvres," *Applied Bionics and Biomechanics*, vol. 7, pp. 41-55, 2010/02/09 2010.
- [13] J. L. Tangorra, et al., "Biorobotic fins for investigations of fish locomotion," in *Intelligent Robots and Systems, 2009. IROS 2009. IEEE/RSJ International Conference on*, 2009, pp. 2120-2125.
- [14] B. E. Flammang and G. V. Lauder, "Speed-dependent intrinsic caudal fin muscle recruitment during steady swimming in bluegill sunfish, *Lepomis macrochirus*," *Journal of Experimental Biology*, vol. 211, pp. 587-598, February 15, 2008.
- [15] B. E. Flammang and G. V. Lauder, "Caudal fin shape modulation and control during acceleration, braking and backing maneuvers in bluegill sunfish, *Lepomis macrochirus*," *Journal of Experimental Biology*, vol. 212, pp. 277-286, January 15, 2009.
- [16] J. A. Mather, et al., "Squid dances: an ethogram of postures and actions of *Sepioteuthis sepioidea* squid with a muscular hydrostatic system," *Marine and Freshwater Behaviour and Physiology*, vol. 43, pp. 45-61, 2010/01/01 2010.
- [17] T. L. Hedrick, "Software techniques for two- and three-dimensional kinematic measurements of biological and biomimetic systems," *Bioinspiration & Biomimetics*, vol. 3, p. 034001, 2008.
- [18] J. L. Tangorra, et al., "The Development of a Biologically Inspired Propulsor for Unmanned Underwater Vehicles," *Oceanic Engineering, IEEE Journal of*, vol. 32, pp. 533-550, 2007.
- [19] J. L. Tangorra, et al., "Biologically derived models of the sunfish for experimental investigations of multi-fin swimming," in *Intelligent Robots and Systems (IROS), 2011 IEEE/RSJ International Conference on*, 2011, pp. 580-587.
- [20] J. L. Tangorra, et al., "The effect of fin ray flexural rigidity on the propulsive forces generated by a biorobotic fish pectoral fin," *Journal of Experimental Biology*, vol. 213, pp. 4043-4054, December 1, 2010.